Cancer Research

Expression of Neuroendocrine Factor VGF in Lung Cancer Cells Confers Resistance to EGFR Kinase Inhibitors and Triggers Epithelial-to-Mesenchymal Transition

Wen Hwang[1], Yu-Fan Chiu[1], Ming-Han Kuo[1], Kuan-Lin Lee[1], An-Chun Lee[1], Chia-Cherng Yu[2], Junn-Liang Chang[3,4], Wen-Chien Huang[5], Shih-Hsin Hsiao[6], Sey-En Lin[7,8], and Yu-Ting Chou[1]

Abstract

Mutations in EGFR drive tumor growth but render tumor cells sensitive to treatment with EGFR tyrosine kinase inhibitors (TKI). Phenotypic alteration in epithelial-to-mesenchymal transition (EMT) has been linked to the TKI resistance in lung adenocarcinoma. However, the mechanism underlying this resistance remains unclear. Here we report that high expression of a neuroendocrine factor termed VGF induces the transcription factor TWIST1 to facilitate TKI resistance, EMT, and cancer dissemination in a subset of lung adenocarcinoma cells. VGF silencing resensitized EGFR-mutated lung adenocarcinoma cells to TKI. Conversely, overexpression of VGF in sensitive cells conferred resistance to TKIs and induced EMT, increasing migratory and invasive behaviors. Correlation analysis revealed a significant association of VGF expression with advanced tumor grade and poor survival in patients with lung adenocarcinoma. In a mouse xenograft model of lung adenocarcinoma, suppressing VGF expression was sufficient to attenuate tumor growth. Overall, our findings show how VGF can confer TKI resistance and trigger EMT, suggesting its potential utility as a biomarker and therapeutic target in lung adenocarcinoma. *Cancer Res; 77(11); 3013–26. ©2017 AACR.*

Introduction

Activating mutations in EGFR constitute one of the major subsets among those molecular aberrations that occur preferentially in patients with clinicopathologic characteristics of lung adenocarcinoma (1–4). EGFR-tyrosine kinase inhibitors (TKI), such as gefitinib, erlotinib, and afatinib, have been shown to produce profound therapeutic responses in lung adenocarcinoma harboring EGFR mutations (exon 19 deletions or the L858R mutation; refs. 5–10). Despite this initial response, patients with EGFR-mutated lung adenocarcinoma ultimately developed resistance to EGFR-TKIs.

A secondary mutation in EGFR (T790M), which abrogates the inhibitory activity of the TKIs, is reported to be the major contributing factor for the development of acquired resistance to EGFR-TKIs (11–13). In contrast, the mutation of T790M infers better survival outcomes and negatively correlates with distant metastasis, thereby predicting a favorable prognosis in lung cancer patients (14–17). New EGFR-TKIs, such as AZD9291 and rociletinib, have been designed to overcome T790M-mediated resistance (18–22). However, treatment of T790M-positive patients with AZD9291 or rociletinib will still eventually develop resistance and in part convert tumors to T790M-negative ones (23, 24). Thus, other non-T790M factors may affect cancer progression and predict worse survival to EGFR-TKI treatment. Pathologic transformation from adenocarcinoma toward the neuroendocrine phenotype similar to small-cell lung cancer or large-cell neuroendocrine carcinoma, has been detected in specimens during EGFR-TKI treatments (13, 25–27). Several studies also revealed that epithelial-to-mesenchymal transition (EMT), a proinvasive phenotype, can endow EGFR-mutated lung cancer cells with EGFR-TKI resistance (28, 29). Nonetheless, the biological mechanism underlying EMT-mediated resistance to EGFR-TKIs remains elusive.

The VGF (nerve growth factor inducible) gene encodes a neuronal and neuroendocrine polypeptide that is secreted by normal neurons and neuroendocrine cells and is responsible for energy balance and metabolism (30, 31). VGF expression enhances neuronal growth and prevents apoptosis (32, 33). VGF has been detected in several neuroendocrine cells and cancers (34–36); however, the role of VGF in tumor progression is not known. In this study, we discovered that VGF is highly expressed in EGFR-TKI–resistant lung adenocarcinoma

[1]Institute of Biotechnology, College of Life Science, National Tsing Hua University, Hsinchu, Taiwan. [2]Department of Medical Research, National Taiwan University Hospital, Taipei, Taiwan. [3]Department of Pathology and Laboratory Medicine, Taoyuan Armed Forces General Hospital, Taoyuan, Taiwan. [4]Department of Biomedical Engineering, Ming Chuan University, Taoyuan, Taiwan. [5]Department of Thoracic Surgery, Mackay Memorial Hospital, Taipei, Taiwan. [6]Division of Pulmonary Medicine, Department of Internal Medicine, Taipei Medical University Hospital, Taipei, Taiwan. [7]Department of Pathology, Taipei Medical University Hospital, Taipei, Taiwan. [8]Department of Pathology, Taipei Municipal Wan Fang Hospital, Taipei, Taiwan.

Note: Supplementary data for this article are available at Cancer Research Online (http://cancerres.aacrjournals.org/).

W. Hwang, Y.-F. Chiu, and M.-H. Kuo are the co-first authors of this article.

Corresponding Author: Yu-Ting Chou, National Tsing Hua University, No. 101, Sec. 2, Kuang-Fu Road, Hsinchu, Taiwan 30013, Republic of China. Phone: 886-3574-2471; Fax: 886-3571-5934; E-mail: ytchou@life.nthu.edu.tw

doi: 10.1158/0008-5472.CAN-16-3168

cells and the expression of VGF induces EMT in EGFR-mutated cells. Therefore, we further characterized the role of VGF in EGFR-TKI resistance and cancer cell dissemination in lung adenocarcinoma.

Materials and Methods

Chemicals and reagents

Gefitinib, erlotinib, afatinib, AZD9291, and rociletinib were purchased from Cayman Chemical. Doxycycline was ordered from Sigma-Aldrich Inc. RPMI1640 and FBS were purchased from GIBCO-BRL.

Cell culture

HCC827 cells were kindly provided by Dr. Jeff Wang (Development Center for Biotechnology, Taiwan) and further certified via short tandem repeat-PCR DNA profiling in 2013 (37). H1975 cells were obtained from Dr. Wayne Chang (National Health Research Institutes, Taiwan) and further authenticated via *EGFR* sequencing analysis in 2015 (38). HCC827GR cells were established in our laboratory, as described in Supplementary Materials and Methods, and tested positive for human origin carrying specific EGFR mutations by *EGFR* sequencing analysis (Supplementary Fig. S1) in 2015. All lung cancer cells were cultured in RPMI1640 medium containing 4 mmol/L L-glutamine, 1 mmol/L sodium pyruvate, 10 mmol/L HEPES, and 10% FBS. Cells were checked routinely and found to be free of contamination by Mycoplasma.

Plasmid construction

The *VGF* was amplified by PCR from cDNA library of HCC827GR cells and then subcloned into HR′-puro plasmid. pLOK.1-shVGF#1 (TRCN0000429075) and pLKO.1-shVGF#2 (TRCN0000180034) were obtained from the National RNAi Core Facility, Academia Sinica (Taipei, Taiwan). pLKO.1-Scrambled shRNA and Tet-PLKO-Puro were obtained from Addgene. Tet-On-shVGF was constructed by inserting a short hairpin double-stranded oligonucleotide targeting VGF into Tet-PLKO-Puro vector and the target sequence is 5′-CTCAGCTCTGAGCATAAAGAG-3′.

Quantitative real-time PCR

Quantitative real-time PCR (qPCR) was performed with specific primers and TaqMan probes or probes from the Universal Probe Library (Roche Applied Science) in the StepOne Real-Time PCR system (Applied Biosystems Inc.). 18S rRNA was used as a reference transcript. Primer sequences designed to detect specific genes and probes are listed in Supplementary Table S1. For quantification of gene copy numbers, total 50 ng genomic DNA extracts from HCC827 and HCC827GR cells were subjected to qPCR analysis with primer sets specific to *EGFR* and *MET* genes. Gene copy numbers from each sample were normalized to *β-actin* (*ACTB)* as a reference gene. Primer sequences and probes were listed in Supplementary Table S2.

Immunoblotting

Cells were harvested in RIPA lysis buffer supplemented with a protease inhibitor cocktail. The antibodies against specific proteins and the titers for immunoblotting and immunofluorescence used in this study are listed in Supplementary Tables S3 and S4, respectively.

Electrical cell substrate impedance sensing assay

Cells (1.0×10^5 per well) were cultured in 400 μL of RPMI with 10% FBS on 8W1E ECIS Cultureware arrays (Applied Biophysics). The arrays were kept in the incubator with 5% CO_2 at 37°C and measured on an ECIS Models Z Theta at multifrequency in 5-minute intervals for 48 hours. Data were analyzed on electrical cell substrate impedance sensing (ECIS) software and normalized to the starting values.

IHC

IHC was conducted as described previously (1, 39). The primary VGF antibody used in the study was VGF antibody (1:300 dilution, GeneTex, catalog no. GTX87831). The immunoreactivity pattern and histologic appearance of all clinical specimens and tissue microarray slides were examined and scored by the pathologist. The Allred scoring system was used to give the staining scores for the expression of VGF based on the sum of the percentage of cells that were stained by IHC (on a scale of 0–5) and the intensity of the staining (on a scale of 0–3).

Animal experiments

Tumor growth assays were conducted as described previously (39). Detailed procedures for the xenograft assays are described in the Supplementary Materials and Methods. All animal experiments were performed in accordance with the animal guidelines of the National Tsing Hua University Institutional Animal Care and approved by Animal Care Committee (permit number: 10260).

Tissue samples and public domain data analysis

The specimens used in IHC were obtained from a high-density tissue array (catalog no. LC2085A, US BIOMAX) of lung tumors or from surgery at Taipei Medical University Hospital. Approval for this study was granted by the Institutional Review Board protocol number CRC-04-11-05. The public gene expression profiling datasets used in this study were analyzed as described previously (38). The sources of these gene expression profiling datasets are listed in Supplementary Table S5. The median levels of specific biomarkers (*VGF*, *CEACAM6*, *SYP*, and *CHGA*) were used as cut-off points for the overall survival analysis.

Statistical analysis

Differences in the IHC staining of human lung cancer specimens were assessed using a Pearson χ^2 test. Associations among the various markers and levels were calculated using Spearman ρ correlation coefficient. Overall survival (OS) curves were generated with Prism 5.0 (GraphPad software Inc.) and estimated by the Kaplan–Meier method. The differences of OS between the high- and low gene–expressing groups were compared by log-rank test. All statistical analyses were performed using SPSS software, version 16 (SPSS, Inc.). A *P* value less than 0.05 was considered to indicate a significant difference.

Results

The molecular events involved during EMT in EGFR-TKI resistance induction

To investigate the mechanism of resistance to EGFR-TKIs in lung cancer, HCC827 cells, which harbor the EGFR delE746_A750 mutation, were treated with an incremental concentration of gefitinib. Surviving cells were pooled together, propagated, and

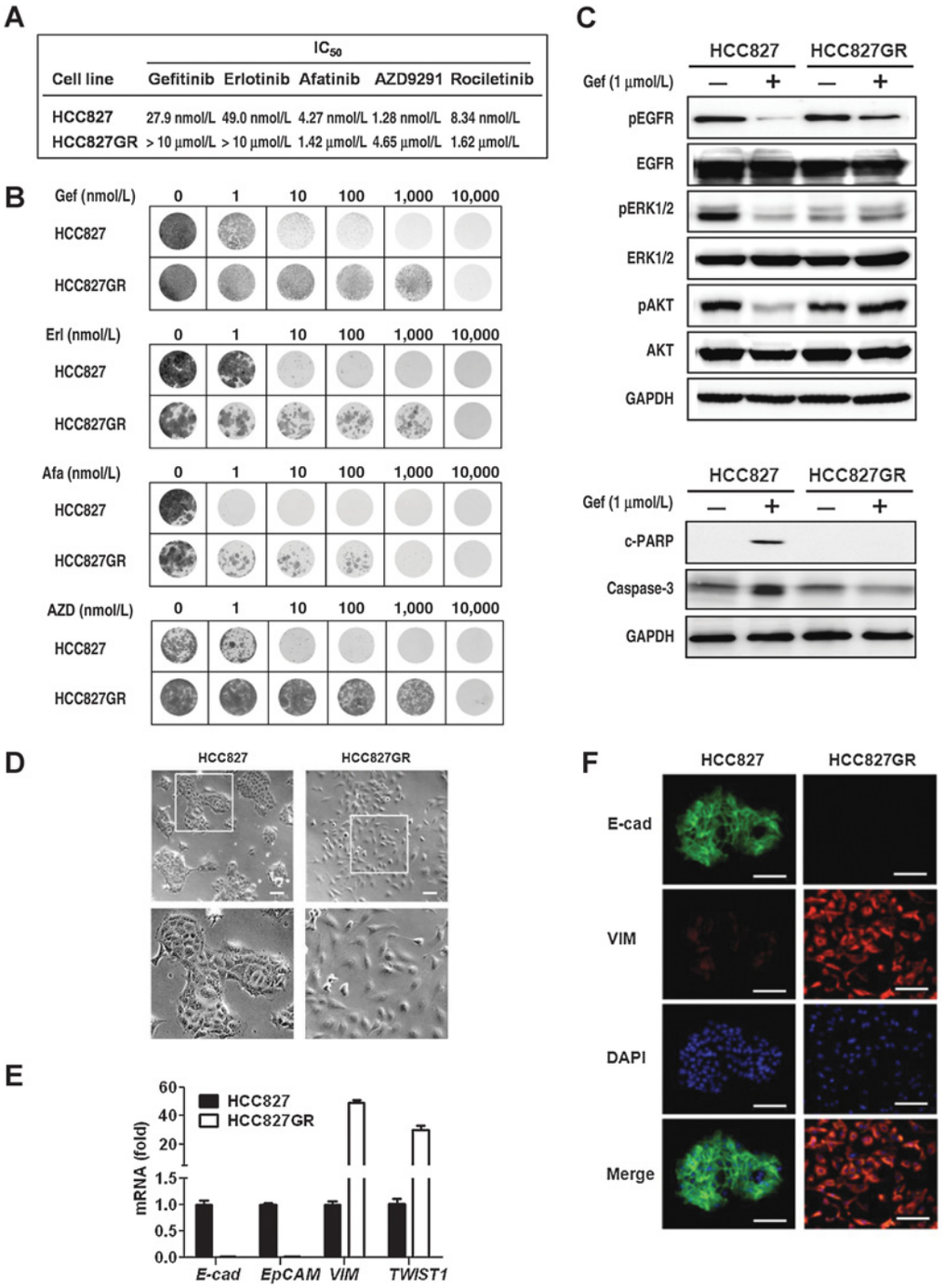

Figure 1.

Development of EGFR-TKI resistance and EMT in lung cancer cells. **A,** IC_{50} analysis of EGFR-TKIs in HCC827 and HCC827GR cells. IC_{50} values of gefitinib, erlotinib, afatinib, AZD9291, and rociletinib were determined in HCC827 and HCC827GR cells via AlamarBlue assay. **B,** Clonogenic analysis of HCC827 and HCC827GR cells treated with indicated concentrations of gefitinib (Gef), erlotinib (Erl), afatinib (Afa), or AZD9291 for 10 days. Photographs represent the growth of HCC827 and HCC827GR cells stained by crystal violet. **C,** Immunoblotting analysis (top) to assess the expression of phosphorylated EGFR (pEGFR), total EGFR (EGFR), phosphorylated ERK1/2 (pERK1/2), total ERK1/2 (ERK1/2), phosphorylated AKT (pAKT), and total AKT (AKT) in both HCC827 and HCC827GR cells treated with or without gefitinib (Gef, 1 μmol/L) for 24 hours. Immunoblotting analysis (bottom) to assess the expression of cleaved PARP and active caspase-3 in HCC827 and HCC827GR cells treated with or without gefitinib (Gef, 1 μmol/L) for 24 hours. **D,** Representative phase-contrast images of HCC827 and HCC827GR cells. Scale bar, 100 μm. **E,** qPCR analysis of *E-cadherin* (*E-cad*), *EpCAM, vimentin* (*VIM*), and *TWIST1* in HCC827GR versus HCC827 cells. **F,** Immunofluorescence analysis to assess the expression of E-cadherin (E-cad, green) and vimentin (VIM, red) in HCC827GR versus HCC827 cells. Nuclei were stained in blue with DAPI. Scale bar, 100 μm.

named HCC827GR cells. The cell viability assay was performed to determine the IC_{50} values of EGFR-TKIs showing that HCC827GR cells were resistant to not only gefitinib but also erlotinib and afatinib (Fig. 1A). Moreover, HCC827GR also exhibited resistance to AZD9291 and rociletinib, the third generation of EGFR-TKIs (Fig. 1A; Supplementary Fig. S2). Consistently, the clonogenic assay demonstrated that HCC827GR cells survived better with EGFR-TKI treatment than HCC827 cells, indicating that HCC827GR cells are resistant to EGFR-TKIs (Fig. 1B). As activation of AKT and ERK (both downstream molecules of EGFR signaling) by phosphorylation is responsible for cellular survival and proliferation, respectively, we examined EGFR, AKT, and ERK phosphorylation in HCC827GR cells as compared with that in HCC827 cells. The immunoblotting assay showed that upon gefitinib treatment, EGFR, AKT, and ERK phosphorylation was attenuated in HCC827, whereas AKT phosphorylation was not diminished by gefitinib in HCC827GR cells as compared with that in HCC827 cells, suggesting the involvement of AKT signaling in EGFR-TKI resistance (Fig. 1C, top). Western blot analysis revealed that gefitinib treatment induced two apoptosis markers, activated caspase-3 and PARP expressions, in HCC827 but not HC827GR cells. These results demonstrated that HCC827GR cells are resistant to gefitinib-induced apoptosis (Fig. 1C, bottom).

HCC827GR cells, though resistant to EGFR-TKIs, neither acquire the mutation of EGFR T790M nor the aberrant expression of MET or HER2 (Supplementary Fig. S1). Phase-contrast image analysis showed that HCC827GR cells exhibited a spindle-like shape in contrast to the epithelial morphology in HCC827 cells (Fig. 1D). The qPCR assay revealed that *E-cadherin* and *EpCAM*, two epithelial markers, were highly expressed in HCC827 but not HCC827GR cells, whereas levels of *vimentin* and *TWIST1*, two mesenchymal markers, were much higher in HCC827GR than those in HCC827 cells (Fig. 1E). In agreement, immunofluorescence staining confirmed the differential expression of cell type–specific markers, E-cadherin and vimentin, between HCC827 and HCC827GR cells (Fig. 1F). These data indicate that induction of EGFR-TKI resistance promotes EMT.

Loss of barrier function and gain of invasion ability in EGFR-TKI–resistant cells

The loss of barrier function is the key cellular event in EMT. Cellular electric resistance (impedance) is determined by cell–cell contact–mediated barrier function (Rb) and cell–matrix interaction (alpha). Electric cell–substrate impedance sensing (ECIS) analysis revealed that after seeding, the level of impedance surged in HCC827, but not HCC827GR cells (Fig. 2A, top left). Moreover, huge elevations in the barrier resistance (Rb) occurred in HCC827, but not HCC827GR cells (Fig. 2A, top right and bottom). These findings indicate the loss of barrier function in HCC827GR cells. Cell tracking and wound-healing assays displayed that HCC827GR cells exhibited better migration and wound-healing abilities than HCC827 cells (Fig. 2B and C). In addition, transwell migration and invasion assays revealed that HCC827GR cells were more migratory and invasive than HCC827 cells (Fig. 2D and E). Our findings indicate the EGFR-TKI–induced EMT facilitates cancer cell dissemination in lung cancer cells.

VGF expression in EGFR-TKI–resistant lung cancer cells

To identify genes involved in EGFR-TKI resistance and EMT processes in lung adenocarcinoma, a gene expression profiling assay followed by qPCR analysis was performed. We found that a gene encoding a neurosecretory polypeptide, *VGF*, is highly elevated in gefitinib-resistant HCC827GR cells as compared with that in the parental HCC827 cells (Fig. 3A, left). The RNA *in situ* hybridization assay confirmed that *VGF* transcript was highly expressed in a primary lung neuroendocrine carcinoma and HCC827GR cells, but not HCC827 cells (Fig. 3A, top right; Supplementary Fig. S3A). Consistent with these findings, *VGF* expression was elevated in the independently isolated EGFR-TKI–resistant HCC827 pool and single-cell clones (Fig. 3B; Supplementary Figs. S4A and S5A S5B). The immunoblotting assay confirmed that more VGF protein was generated in HCC827GR than in HCC827 cells (Fig. 3A, bottom right). In agreement, the immunomagnetic reduction assay displayed that HCC827GR cells secreted more VGF than HCC827 cells in the conditioned medium (Supplementary Fig. S6A). We further examined *VGF* expression in primary tumors and cell lines derived from different pathologic types of lung cancer. We observed that *VGF* levels were higher in pulmonary neuroendocrine tumors, such as small-cell lung cancer and large-cell neuroendocrine carcinoma, than adenocarcinoma and squamous cell carcinoma, while a few of adenocarcinoma cells exhibited high levels of *VGF* expression (Fig. 3C; Supplementary Figs. S7 and S8). To examine whether *VGF* levels are associated with EGFR-TKI–resistant status in lung cancer cells, the IC_{50} values of gefitinib in different EGFR-mutated lung adenocarcinoma cell lines were determined (Fig. 3D, left). qPCR analysis revealed that *VGF* levels were low in EGFR-TKI–sensitive cells but high in resistant cells (Fig. 3D, right; Supplementary Fig. S9). Moreover, in single-cell clones selected from gefitinib-treated HCC827 cells, *VGF* levels positively correlated with IC_{50} values of gefitinib and EMT marker expression (Supplementary Fig. S5). These data suggest a possible association between *VGF* expression and EGFR-TKI resistance in lung adenocarcinoma cells. Intriguingly, *VGF* transcript was detected in H1975, a cell line harboring EGFR L858R/T790M double mutations (Supplementary Fig. S3B). We found that H1975 was more resistant to afatinib than its *VGF*-low counterpart (Supplementary Fig. S10). Moreover, we observed that VGF was expressed in not only treatment-naïve lung neuroendocrine carcinoma (case 1) but also acquired EGFR-TKI resistant lung adenocarcinomas (case 2 and case 3), suggesting the involvement of *VGF* expression in EGFR-TKI resistance (Fig. 3E). To study the role of *VGF* in EGFR-TKI resistance, *VGF* was knocked down in HCC827GR cells, followed by gefitinib-mediated cell viability analysis (Fig. 3F). The cell viability assay revealed that *VGF* silencing rendered HCC827GR cells sensitive to gefitinib (Fig. 3F, lower). These data indicate that *VGF* is critical for the maintenance of EGFR-TKI resistance.

VGF prevents EGFR-TKI–induced apoptosis

To further elucidate the role of *VGF* in EGFR-TKI resistance, we ectopically expressed *VGF* in HCC827 cells (Fig. 4A). The cell viability assay demonstrated that VGF expression increased the IC_{50} values of various EGFR-TKIs in the HCC827 cells (Fig. 4B). Consistently, clonogenic analysis showed that *VGF* expression endowed the HCC827 cells with enhanced EGFR-TKI resistance, indicating that *VGF* expression enhances EGFR-TKI resistance in lung cancer cells (Fig. 4C; Supplementary Fig. S2). We further investigated the effect of EGFR-TKI treatment on the phosphorylation of EGFR, ERK, or AKT in *VGF*-expressing HCC827 cells. Immunoblotting revealed that gefitinib treatment attenuated the phosphorylation of AKT in the control HCC827 cells, but

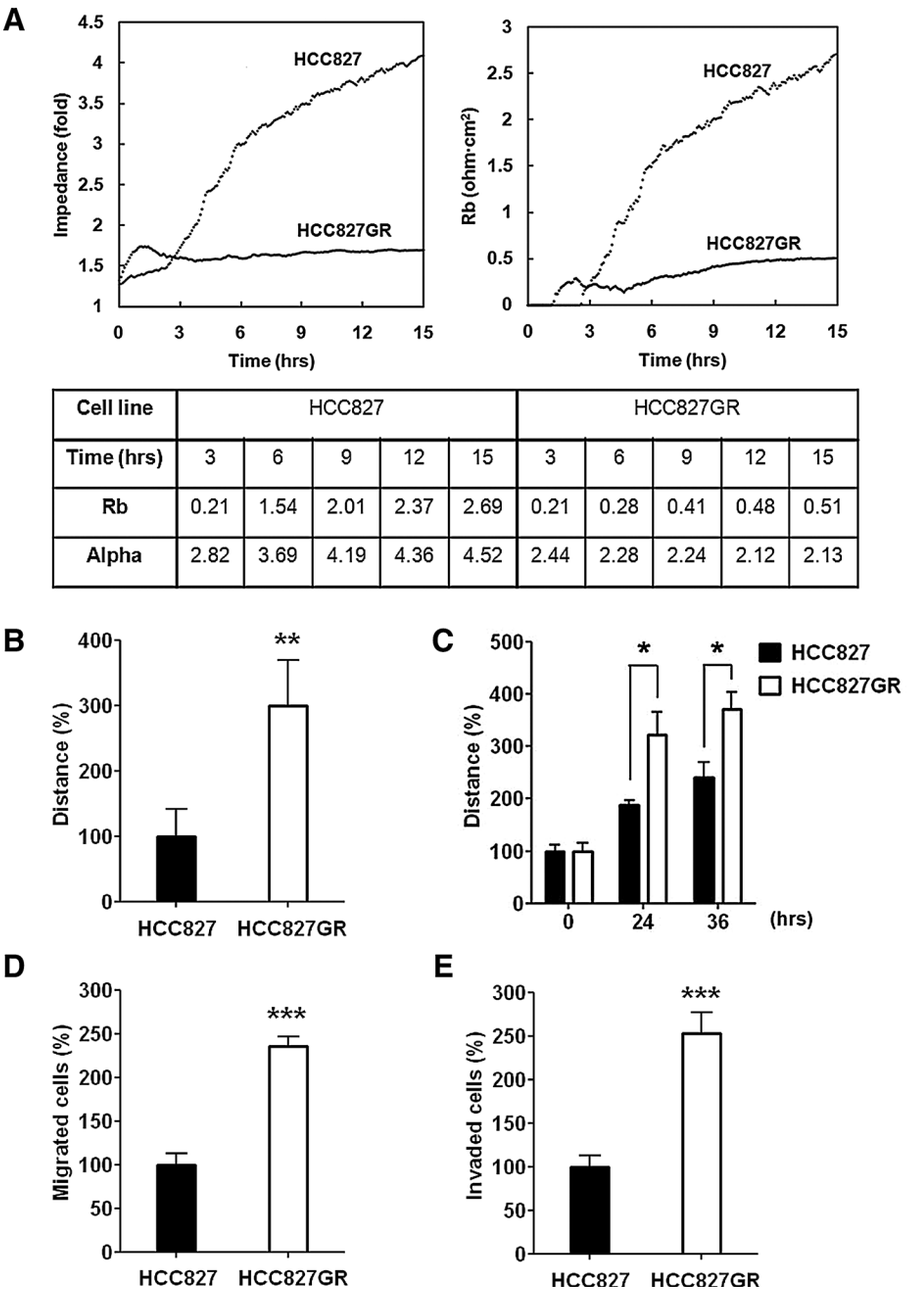

Cell line	HCC827					HCC827GR				
Time (hrs)	3	6	9	12	15	3	6	9	12	15
Rb	0.21	1.54	2.01	2.37	2.69	0.21	0.28	0.41	0.48	0.51
Alpha	2.82	3.69	4.19	4.36	4.52	2.44	2.28	2.24	2.12	2.13

Figure 2.

Decreased barrier function and enhanced invasive ability in EGFR-TKI–resistant cells. **A,** ECIS analysis to measure the changes of impedance (top left) and Rb (top right) in HCC827GR versus HCC827 cells. The representative values of Rb and alpha, which monitor the changes of barrier function and cell–extracellular matrix interaction, respectively, are listed (bottom). **B,** Cell tracking analysis to measure the relative migratory distance of HCC827GR versus HCC827 cells during 24 hours. Statistical significance, **, $P < 0.01$. **C,** Wound-healing assay of HCC827 and HCC827GR cells. Statistical significance, *, $P < 0.05$. **D,** Transwell migration assay of HCC827 and HCC827GR cells. Statistical significance, ***, $P < 0.001$. **E,** Transwell invasion analysis of HCC827 and HCC827GR cells. Statistical significance, ***, $P < 0.001$.

not in *VGF*-expressing HCC827 cells (Fig. 4D, top). Moreover, gefitinib treatment induced the expression of cleaved PARP and activated caspase-3 in control but not *VGF*-expressing HCC827 cells (Fig. 4D, bottom). As EMT regulators, such as TWIST1, SLUG, and SNAIL, have been reported to regulate cell survival, we further examined their expression in HCC827 and HCC827GR cells (40). qPCR analysis revealed that *TWIST1*, but not *SLUG* and *SNAIL*, was highly expressed in HCC827GR cells (Fig. 4E; Supplementary Fig. S11A). Correlation analysis showed that *VGF* expression was closely associated with *TWIST1* levels in primary lung adenocarcinoma (Supplementary Fig. S11B). Moreover, we confirmed that *VGF* expression induced *TWIST1* in HCC827 cells (Fig. 4E). We further examined the effect of TWIST1 on EGFR-TKI resistance. Clonogenic analysis displayed that TWIST1 expression endowed HCC827 cells with EGFR-TKI resistance (Fig. 4F; Supplementary Fig. S11C). These data indicate that VGF-TWIST1 signaling encourages EGFR-TKI resistance in EGFR-mutated lung cancer cells.

VGF induces EMT and cancer cell dissemination

Because the above data suggest that VGF expression enhances EGFR-TKI resistance, which induces EMT, we further examined the effect of VGF expression on EMT and cancer cell dissemination. Phase-contrast image analysis showed that the *VGF* expression induced a morphologic change from an epithelial to a spindle-like phenotype (Fig. 5A). qPCR and immunoblotting

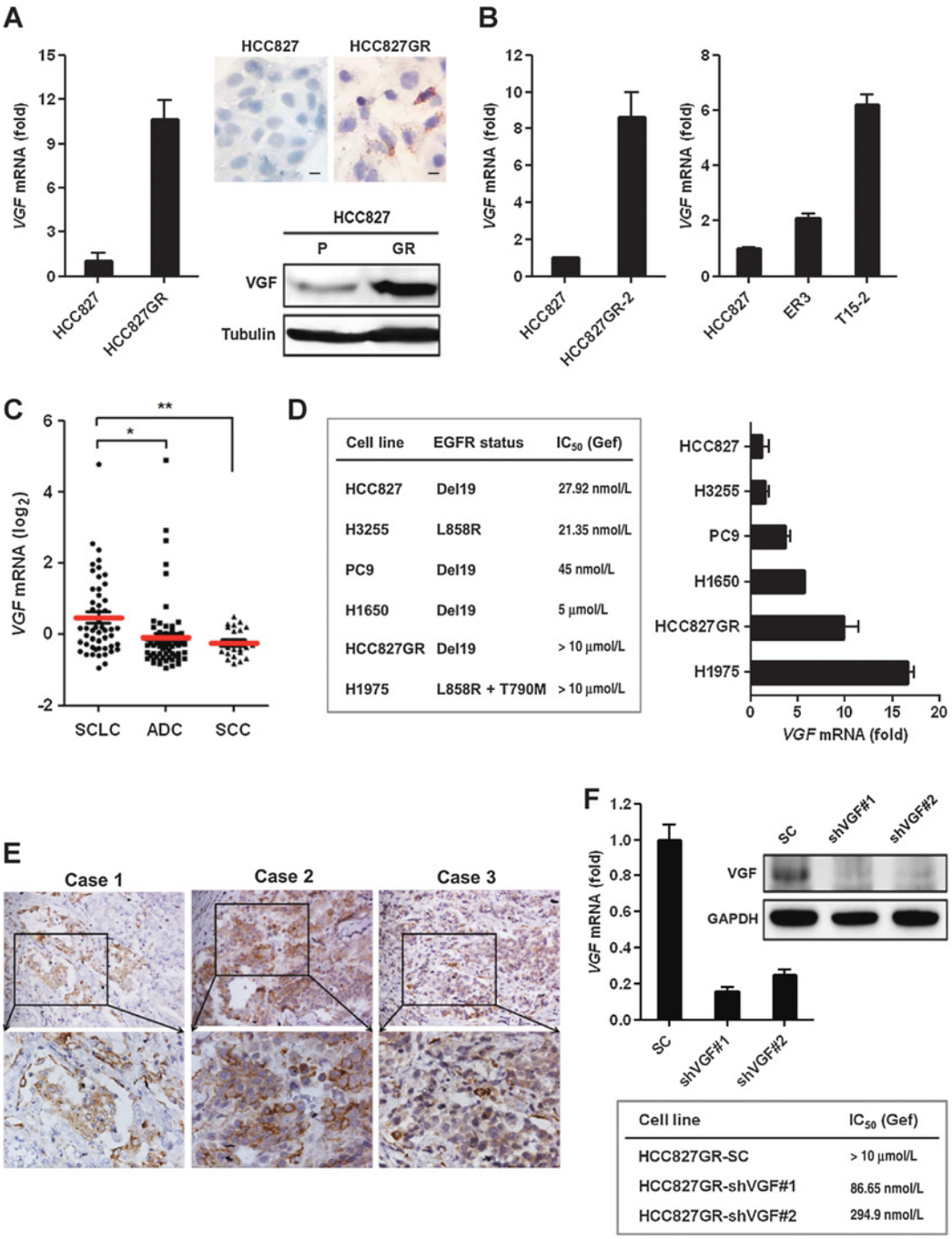

Figure 3.

Expression of VGF in EGFR-TKI–resistant lung cancer cells. **A,** qPCR analysis (left) and the RNA *in situ* hybridization assay (top right) to assess *VGF* transcript expression in HCC827GR versus HCC827 cells. Immunoblotting (bottom right) of VGF protein expression in HCC827GR versus HCC827 cells. Tubulin served as a loading control. Scale bar, 10 μm. **B,** qPCR analysis (left) of *VGF* expression in HCC827GR-2, an independently selected EGFR-TKI–resistant HCC827 pool versus HCC827 cells. Gene expression analysis (right) of *VGF* expression in HCC827- and EGFR-TKI–resistant clones (ER3 and T15-2) from the database of GSE38310. **C,** Gene expression analysis of *VGF* expression in different pathologic types of lung cancer cell lines from the database of TCGA_CCLE. SCLC, small-cell lung cancer; ADC, adenocarcinoma; SCC, squamous cell carcinoma. Statistical significance, *, $P < 0.05$; **, $P < 0.01$. **D,** List of IC_{50} of gefitinib and EGFR mutations status (left) and qPCR analysis (right) of *VGF* expression in the indicated lung adenocarcinoma cell lines. **E,** IHC analysis of VGF expression in three cases of lung cancer. Case 1: treatment-naïve neuroendocrine carcinoma; case 2 and case 3: acquired EGFR-TKI resistant lung adenocarcinomas harboring EGFR Del19/T790M mutations (top, ×200; bottom, ×400). **F,** qPCR analysis (left) and Western blotting (top right) to assess *VGF* expression in HCC827GR cells infected with lentiviral vectors encoding shVGF or scrambled control (SC). shVGF#1 and shVGF#2 target different regions in *VGF* mRNA. The AlamarBlue assay (bottom) to assess the viability of HCC827 and HCC827GR cells infected with lentiviral vectors encoding shVGF or SC, followed by treatment with different gefitinib (Gef) concentrations for 3 days.

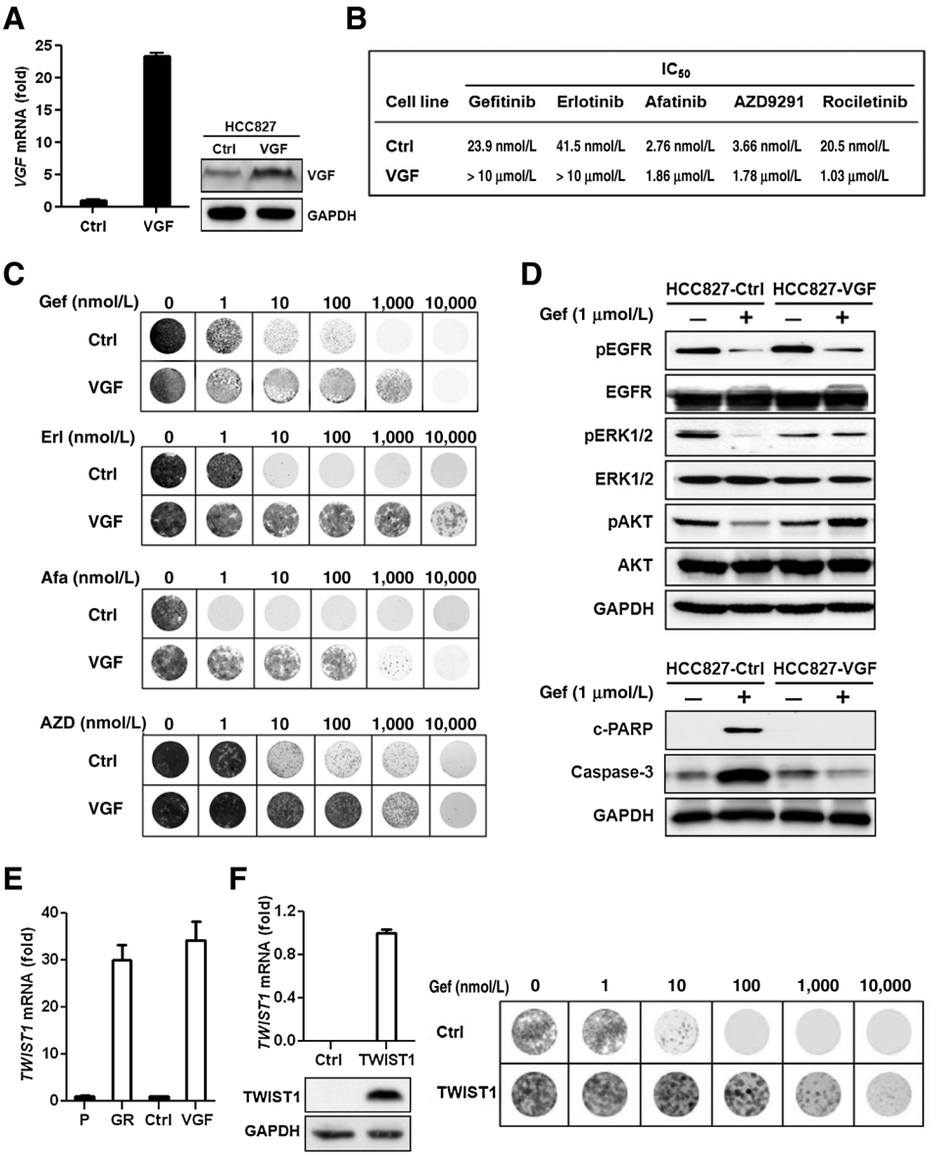

Figure 4.

VGF induces TWIST1 and encourages EGFR-TKI resistance. **A,** qPCR analysis (left) and immunoblotting (right) for *VGF* expression in HCC827 cells infected with the lentiviral vector encoding cDNA of *VGF* (HCC827-VGF) or empty control vector (HCC827-Ctrl). GAPDH served as a loading control. **B,** IC_{50} analysis of EGFR-TKIs. IC_{50} values of gefitinib, erlotinib, afatinib, AZD9291, and rociletinib in HCC827-Ctrl and HCC827-VGF cells were determined via AlamarBlue assay. **C,** Clonogenic analysis of HCC827-Ctrl and HCC827-VGF cells treated with indicated concentrations of gefitinib (Gef), erlotinib (Erl), afatinib (Afa), or AZD9291 (AZD) for 10 days. Photographs represent growth of both HCC827-Ctrl and HCC827-VGF cells stained by crystal violet. **D,** Immunoblotting analysis (top) to assess the expression of phosphorylated EGFR (pEGFR), total EGFR (EGFR), phosphorylated ERK1/2 (pERK1/2), total ERK1/2 (ERK1/2), phosphorylated AKT (pAKT), and total AKT (AKT) in HCC827-Ctrl and HCC827-VGF cells treated with or without gefitinib (1 μmol/L) for 24 hours. Immunoblotting analysis (bottom) to assess the expression of apoptotic markers, cleaved PARP, and active caspase-3 in HCC827-Ctrl and HCC827-VGF cells treated with or without gefitinib (1 μmol/L) for 24 hours. **E,** qPCR analysis of *TWIST1* expression in HCC827GR versus HCC827 and HCC827-VGF versus HCC827-Ctrl cells. **F,** qPCR (top left) and immunoblotting (bottom left) analyses of *TWIST1* expression in HCC827 cells infected with lentiviral vector encoding cDNA of *TWIST1* (HCC827-TWIST1) or empty control vector (HCC827-Ctrl). Clonogenic analysis (right) of HCC827-Ctrl and HCC827-TWIST1 cells treated with indicated gefitinib (Gef) concentrations for 10 days. Photographs represent growth of HCC827-Ctrl and HCC827-TWIST1 cells stained by crystal violet.

assays revealed that ectopic expression of *VGF* attenuated the expression of *E-cadherin* and *EpCAM* but elevated the levels of *vimentin* and *TWIST1* (Fig. 5B and D). Immunofluorescence staining demonstrated that the *VGF* expression induced a switch from E-cadherin to vimentin in the HCC827 cells, supporting that *VGF* induces EMT (Fig. 5C). ECIS analysis displayed that VGF expression diminished impedance (Fig. 5E, top left) and attenuated Rb levels in HCC827, indicating a loss of barrier function in *VGF*-expressing cells (Fig. 5E, top right and bottom). The transwell assay revealed that VGF expression promoted migration and

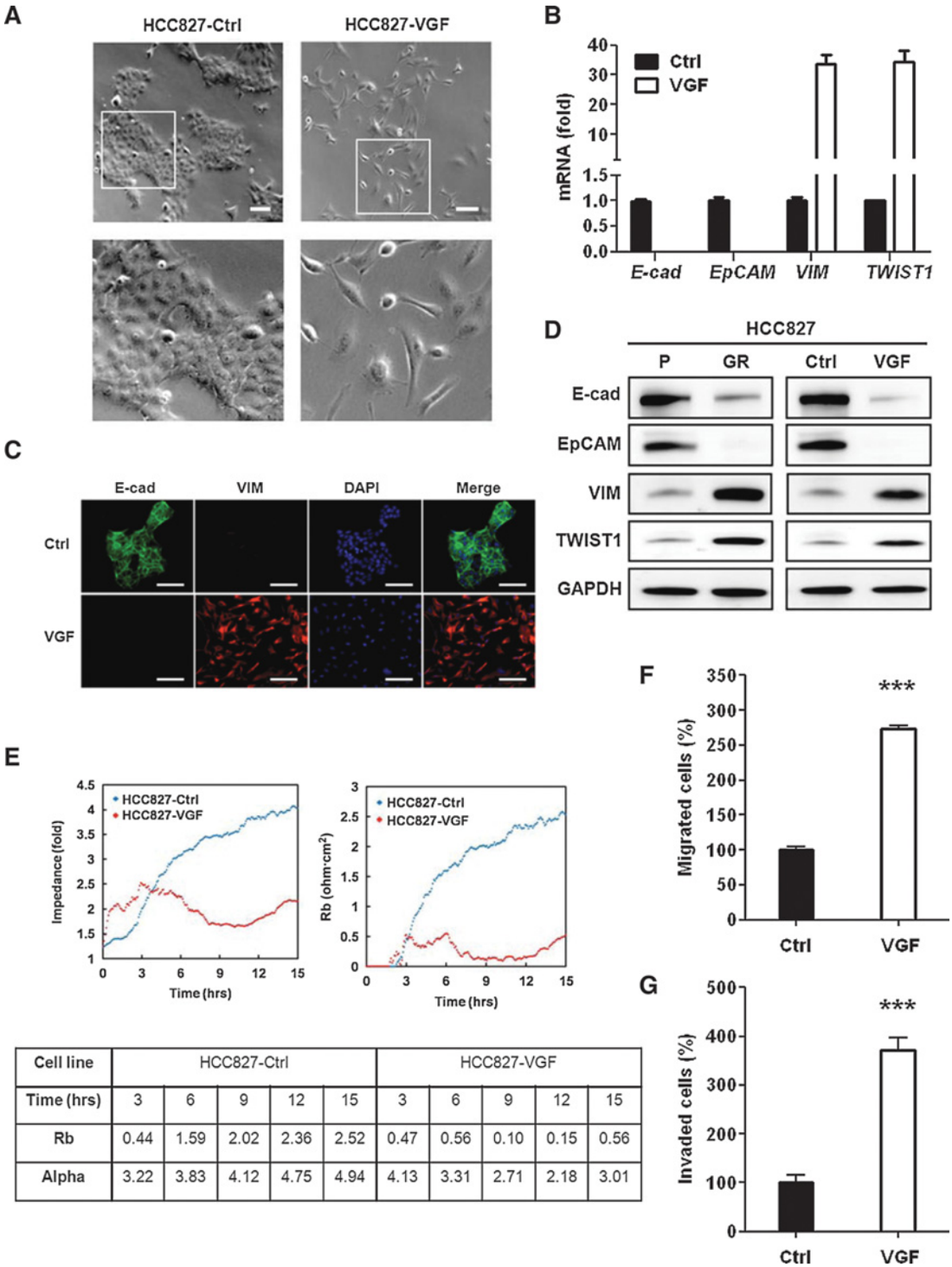

Cell line	HCC827-Ctrl					HCC827-VGF				
Time (hrs)	3	6	9	12	15	3	6	9	12	15
Rb	0.44	1.59	2.02	2.36	2.52	0.47	0.56	0.10	0.15	0.56
Alpha	3.22	3.83	4.12	4.75	4.94	4.13	3.31	2.71	2.18	3.01

Figure 5.

VGF induces EMT and cancer cell dissemination. **A,** Representative phase-contrast images of HCC827 cells infected with the lentiviral vector encoding cDNA of *VGF* (HCC827-VGF) or empty control vector (HCC827-Ctrl). Scale bar, 100 μm. **B,** qPCR analysis of *E-cadherin* (*E-cad*), *EpCAM*, TWIST1, and *vimentin* (*VIM*) expression in HCC827-Ctrl and HCC827-VGF cells. **C,** Immunofluorescence of E-cadherin (E-cad; green) and vimentin (VIM; red) expression in HCC827-Ctrl (Ctrl) and HCC827-VGF (VGF) cells. Nuclei were stained in blue with DAPI. Scale bar, 100 μm. **D,** Immunoblotting analysis in parental HCC827 (P), HCC827GR (GR), HCC827-Ctrl (Ctrl), and HCC827-VGF (VGF) cells to assess the expression of E-cadherin (E-cad), EpCAM, vimentin (VIM), and TWIST1. GAPDH served as a loading control. **E,** ECIS analysis to monitor the changes of impedance (top left) and Rb (top right) in HCC827-VGF versus HCC827-Ctrl cells. The representative Rb and alpha values are listed (bottom). **F,** Transwell migration assay of HCC827-Ctrl and HCC827-VGF cells. Statistical significance, ***, $P < 0.001$. **G,** Transwell Matrigel invasion analysis of HCC827-Ctrl and HCC827-VGF cells. Statistical significance, ***, $P < 0.001$.

invasion in lung cancer cells (Fig. 5F and G). As VGF induces TWIST1, we further examined the effect of TWIST1 on cancer cell dissemination. Ectopic expression of TWIST1 induced a spindle-like morphologic change in HCC827 cells accompanied with the increased expression of mesenchymal markers, such as *vimentin* and *N-cadherin* (Supplementary Fig. S11D and S11E). Moreover, cell-tracking analysis revealed that TWIST1 expression encouraged cell migration (Supplementary Fig. S11F). Our findings support that VGF-TWIST1 signaling induces EMT and lung cancer cell dissemination.

VGF silencing attenuates tumor growth

To evaluate the biological significance of elevated endogenous *VGF* in EGFR-TKI resistant cells, we knocked down the *VGF* expression and measured its effect on lung cancer cell growth. Clonogenic assays showed that the knockdown of *VGF* attenuated cell growth in the EGFR-TKI–resistant cell lines HCC827GR and H1975 (Fig. 6A). Treatment of *VGF*-silenced HCC827GR cells with the condition medium from *VGF*-transfected HEK293T cells rescued cells from growth arrest (Supplementary Fig. S6B). Clonogenic analysis revealed that VGF-positive lung cancer cell lines, including HCC827GR, H1975, and H1299, were more resistant to the low serum (1% FBS) condition than VGF-negative HCC827 (Supplementary Fig. S12A and S12B). Moreover, overexpression of VGF in HEK293T endowed cells with an increased cell survival capacity under the low serum condition (Supplementary Fig. S12C). We observed that conditioned media from HCC827GR or *VGF*-expressing cells enhanced growth of HCC827 under low serum stress (Supplementary Fig. S12D). These findings suggest that *VGF* is essential for cell growth and survival *in vitro*. To evaluate the importance of *VGF* in maintaining cell growth *in vivo*, *VGF* was knocked down in HCC827GR cells prior to subcutaneous injection into a xenograft nude mouse tumor model. The HCC827GR cells formed tumors readily in this xenograft animal model; however, knockdown of VGF diminished tumor growth, indicating that the VGF expression enhances tumor growth *in vivo* (Fig. 6B). We further generated HCC827GR/tet-on-shVGF cells in which doxycycline induces shVGF expression to silence *VGF* (Fig. 6C; Supplementary Fig. S13A). The clonogenic assays showed that doxycycline treatment attenuated cell growth in HCC827GR/tet-on-shVGF but not in control HCC827GR/tet-on cells (Fig. 6C; Supplementary Fig. S13A). To further test whether VGF could function as a therapeutic target, HCC827GR/tet-on-shVGF cells were subjected to a xenograft animal assay. When palpable tumor bulges were observed in the host mice, shVGF was induced by doxycycline treatment in the xenograft tumors. We found that doxycycline-induced knockdown of endogenous *VGF* attenuated tumor growth in HCC827GR/tet-on-shVGF cells, causing decrease of tumor weight, and doxycycline alone had no effect on tumor growth in HCC827GR/tet-on control cells (Fig. 6D; Supplementary Fig. S13B). Our findings support the notion that *VGF* is essential for oncogenic tumor growth and is a potential therapeutic target in lung cancer.

VGF correlates with advanced tumor grade and poor survival in lung adenocarcinoma

To characterize the role of VGF in the tumor progression of lung cancer, we measured VGF expression in lung adenocarcinoma by IHC analysis of a panel of 70 specimens. IHC staining revealed that VGF was preferentially expressed in poorly differentiated (75% grade III) lung adenocarcinomas as compared with well (25% grade I) and moderately differentiated (30% grade II) ones, and a χ^2 analysis indicated that the association of VGF expression with pathologic grades was significant ($P = 0.001$; Fig. 7A). The aforementioned data indicated that VGF induced EMT in lung cancer cells. In primary lung adenocarcinoma, we further validated the correlation of *VGF* with EMT markers. Correlation analysis demonstrated the presence of a positive correlation of *VGF* with *VIM*, *N-cadherin*, and *TWIST1* (Fig. 7B; Supplementary Fig. S14A and S14B). Because CEACAM6 is currently used as a biomarker for diagnosis and prognosis in lung adenocarcinoma (41), we further examined its expression in EGFR-TKI–resistant versus sensitive cells. The qPCR assay revealed that the expression of *CEACAM6* was lost in EGFR-TKI resistant cells, such as HCC827GR and the independently selected cells (ER3, T15-2), as compared with that in the parental HCC827 cells (Supplementary Fig. S14C). Correlation analysis revealed that *VGF* negatively correlated with *CEACAM6* (Supplementary Fig. S14D). Kaplan–Meier survival analysis was then conducted for lung adenocarcinoma to determine the prognostic significance of the expression of *VGF* versus *CEACAM6*. In lung adenocarcinoma, we found that *VGF* expression correlated with poor survival; in contrast, the expression of *CEACAM6* and neuroendocrine markers, such as *Chromogranin A*, *Chromogranin B*, and *Synaptophysin*, did not correlate with survival outcome (Fig. 7C; Supplementary Fig. S15). Moreover, tumors harboring a $VGF^{high}/TWIST1^{high}$ signature were associated with worse survival as compared with those carrying a $VGF^{low}/TWIST1^{low}$ signature (Fig. 7C, right). Consistently, in EGFR-mutated lung adenocarcinoma, we observed that *VGF* expression predicted poor survival, whereas *CEACAM6* expression did not correlate with the survival outcome (Fig. 7D, left and middle; and Supplementary Fig. S16). In EGFR-mutated lung adenocarcinoma, we observed that a $VGF^{high}/TWIST1^{high}$ signature predicted a worse prognosis than a $VGF^{low}/TWIST1^{low}$ signature (Fig. 7D, right; Supplementary Fig. S16). These data indicate the potential of *VGF* and *TWSIT1* as prognostic biomarkers for lung adenocarcinoma.

Discussion

Although EMT has been linked to EGFR-TKI resistance, the mechanism is not clear. In this study, we found that VGF, a neuroendocrine factor, is highly expressed in EGFR-TKI–resistant lung adenocarcinoma cells, the growth of which is dependent on VGF expression. The ectopic expression of VGF supports cell growth with EGFR-TKI resistance and induces EMT. Our findings revealed for the first time that VGF functions as an emerging factor in EGFR-TKI resistance and EMT in lung adenocarcinoma.

VGF was originally identified in the neurons and neuroendocrine cells and is responsible for normal metabolism as well as cell survival and proliferation in the hippocampus (30, 42). Moreover, VGF was reported to protect neuron cells from ER stress–induced cell death, suggesting its involvement in stress-induced cell survival (33). In lung cancer, VGF was first detected in neuroendocrine lung carcinoma cell lines by proteomic analysis, while the biological and clinical significance of VGF in tumors have not been known (35). In this study, we found that *VGF* is highly expressed in EGFR-TKI–resistant cells. We discovered that *VGF* expression activates AKT survival signaling, thus preventing the cells from undergoing EGFR-TKI–induced apoptosis in lung

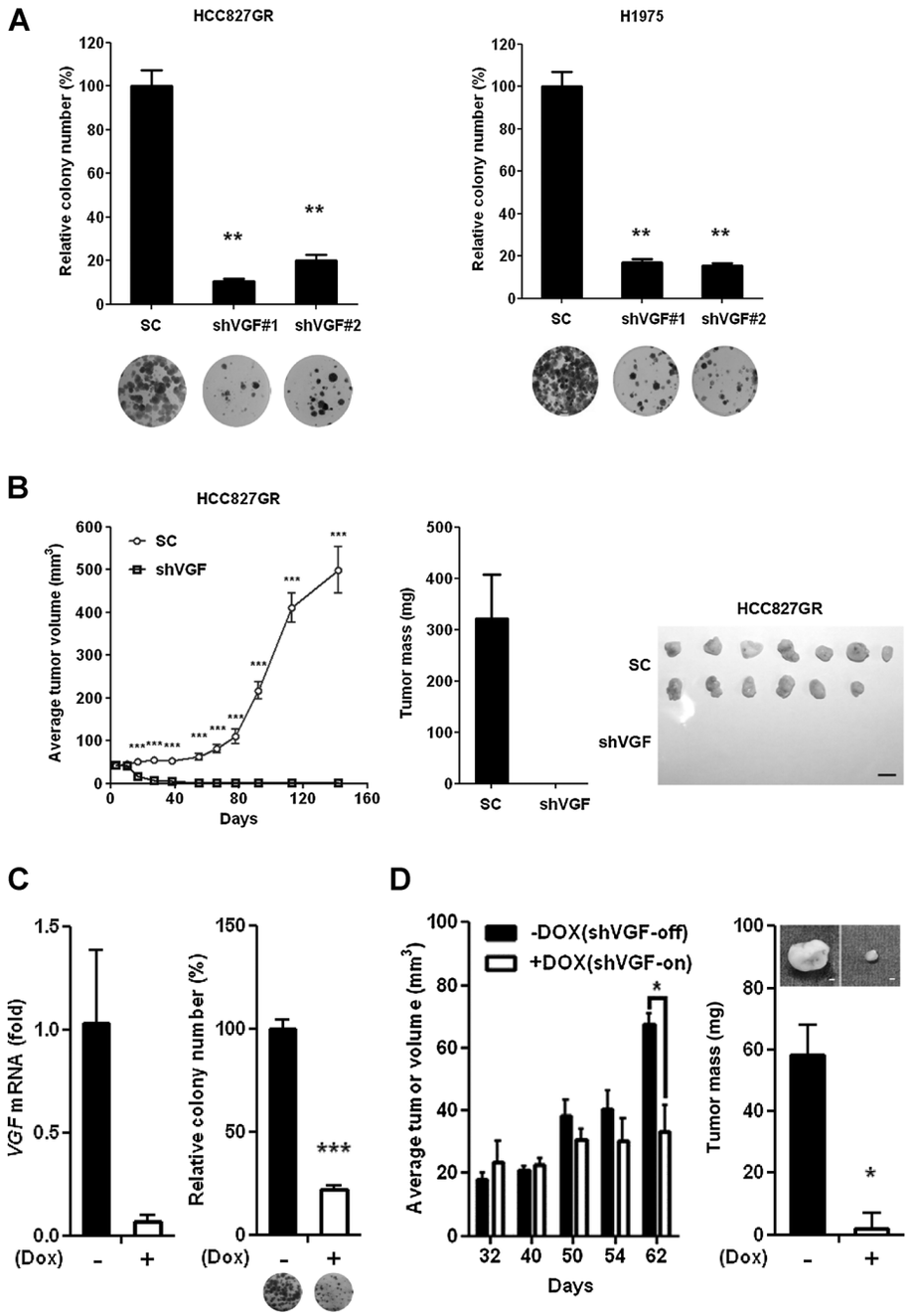

Figure 6.

VGF silencing attenuates tumor cell growth *in vitro* and *in vivo*. **A,** The clonogenic assay to assess the effect of *VGF*-silencing on EGFR-TKI–resistant HCC827GR (left) and H1975 (right) lung cancer cells. HCC827GR and H1975 cells were infected with lentiviral vector encoding shVGF (shVGF) or scrambled control (SC) and subjected to clonogenic analysis. shVGF#1 and shVGF#2 target different regions in *VGF* mRNA. Photographs represent growth of cells stained by crystal violet. Statistical significance, **, $P < 0.01$. **B,** Xenograft assay for assessing the effect of *VGF* silencing on tumor growth. HCC827GR cells were infected with lentiviral vector encoding shVGF (shVGF) or scrambled control (SC) and subjected to Trypan blue viability assay. Survived cells were further injected subcutaneously into nude mice. Tumor volume was monitored over time as indicated (left). Tumor weights (middle) were measured after harvest. The representative photographs (right) illustrate tumor growth 140 days after injection. Scale bar, 10 mm. Error bars, SEM ($n = 7$ mice/group; ***, $P < 0.001$). **C,** qPCR analysis (left) and clonogenic assay (right) to assess the *VGF* expression and effect of *VGF* silencing, respectively, in HCC827GR/tet-on-shVGF cells in which shVGF was induced by doxycycline (Dox). HCC827GR cells were stably transfected with pLKO-tet-on-shVGF, which encodes a doxycycline-inducible shVGF, to generate HCC827GR/tet-on-shVGF cells in which endogenous *VGF* levels could be downregulated by treatment with doxycycline. Photographs (bottom right) represent the growth of cells stained by crystal violet. Statistical significance, ***, $P < 0.001$. **D,** Xenograft assay to assess the effect of *VGF* silencing on tumor growth. HCC827GR/tet-on-shVGF cells were injected subcutaneously into nude mice. Thirty-two days after cancer cell injection, mice were treated with or without daily oral doxycycline for another 30 days. Tumor volume was monitored over time as indicated (left). Tumor weight was measured after harvest (bottom right). The representative photographs illustrate tumor growth 30 days after doxycycline or normal saline treatment (top right). Scale bar, 1 mm. Error bars, SEM ($n = 6$ mice/group; *, $P < 0.05$).

A

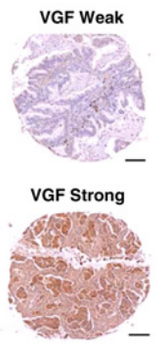

Histologic grade and VGF expression (lung adenocarcinoma)

VGF Expression	Histologic grade		
	I	II	III
VGF Weak/negative	15 (75%)	21 (70%)	5 (25%)
VGF Strong/positive	5 (25%)	9 (30%)	15 (75%)
Total	20	30	20

B

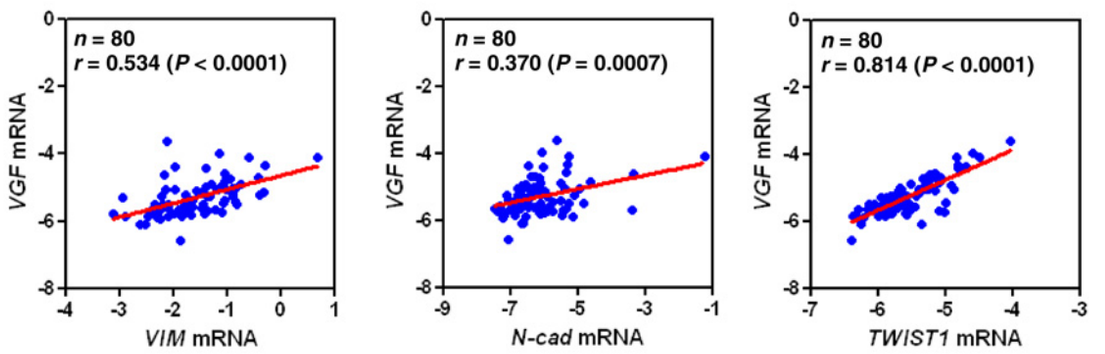

C

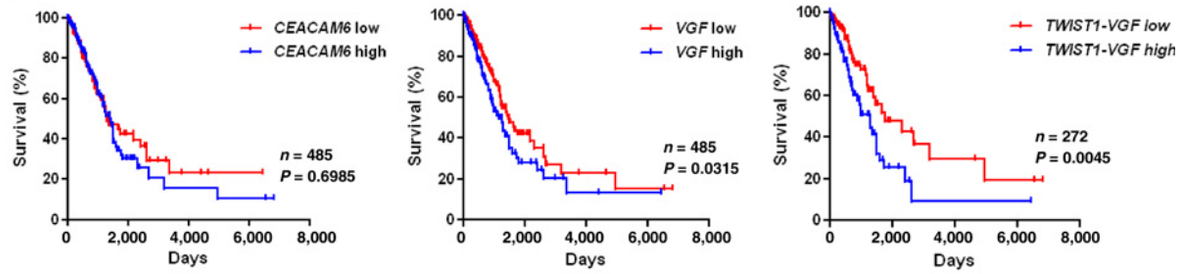

D

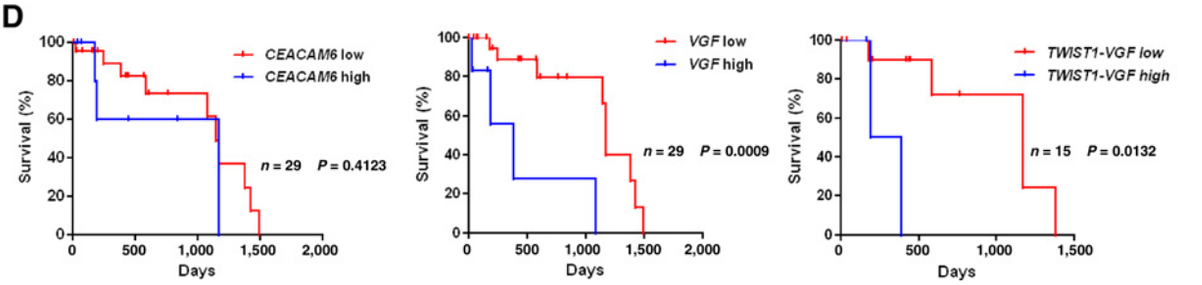

Figure 7.

VGF expression correlates with tumor malignancy in lung adenocarcinoma. **A,** Representative IHC staining (left) of weak and strong VGF expression in lung adenocarcinoma. Scale bar, 200 μm. χ^2 analysis (right) for correlation between VGF expression and tumor grades in lung adenocarcinoma. **B,** Scatter plots generated from primary lung adenocarcinoma (GSE43458) displaying positive correlations between *VGF* and EMT markers, *vimentin* (*VIM*), *N-cadherin* (*N-cad*), and *TWIST1* (Spearman correlation analysis). **C,** Kaplan–Meier analysis to assess the correlation of *CEACAM6* (left) or *VGF* (middle) expression with the overall survival of primary lung adenocarcinoma from the The Cancer Genome Atlas (LUAD) database. The overall survival data were further stratified by $VGF^{high}/TWIST1^{high}$ and $VGF^{low}/TWIST1^{low}$ signatures for Kaplan–Meier analysis (right). Comparative analysis by log-rank test was performed between the different groups. **D,** Kaplan–Meier analysis to assess the correlation of *CEACAM6* (left) or *VGF* (middle) expression with the overall survival of EGFR-mutated lung adenocarcinoma from the The Cancer Genome Atlas (LUAD) database. Comparative analysis by log-rank test was performed between the different groups.

adenocarcinoma cells. We found that VGF-containing conditioned media can promote cell growth in the low serum culture (Supplementary Figs. S6 and S12); moreover, *VGF* silencing in HCC827GR cells attenuates tumor cell growth both *in vitro* and *in vivo* (Fig. 6). These data support a critical role of *VGF* in growth and survival in VGF-positive lung cancer cells. Thus, we propose that VGF-induced survival signaling is essential for the development of acquired EGF-TKI resistance in both T790M-dependent and independent mechanisms. In support of this hypothesis, we observed that VGF is highly expressed in the case 2 and case 3 of T790M-positive lung adenocarcinomas, which were treated with EGFR-TKIs before (Fig. 3E). Consistently, we found that H1975, harboring EGFR L858R/T790M mutations, exhibits a high level of *VGF*, and H1975 is more resistant to afatinib and expresses lower E-cadherin than its VGF^{low} counterpart (Supplementary Fig. S10). Moreover, the knockdown of *VGF* in H1975 attenuates cell growth (Fig. 6A), supporting the notion that VGF expression promotes EGFR-TKI resistance, EMT, and cell growth. As described in the ATCC database, H1975 lung adenocarcinoma cell line was established by Adi Gazdar and John Milnor from a female nonsmoker in 1988, prior to the clinical use of TKIs. Thus, high VGF expression in EGFR-mutated lung tumors cannot all be attributed to the acquired resistance of EGFR-TKI treatment, but may, in part, naturally exist before the selection. In support of this view, VGF is highly expressed in the case 1 of lung neuroendocrine carcinoma, which harbors wild-type EGFR and was never treated with EGFR-TKIs (Fig. 3E). We observed that VGF-positive lung cancer cells, such as HCC827GR, H1975, and H1299, are more resistant to low serum stress and EGFR-TKI treatment than VGF-negative HCC827, whereas H1975 and H1299 were derived from patients never treated with EGFR-TKIs (Supplementary Fig. S12A and S12B). Our *in vitro* and *in vivo* animal models indicated that VGF silencing inhibits cancer cell growth and tumor formation, suggesting that VGF contains oncogenic properties with the potential to serve as a therapeutic target (Fig. 6). New modalities targeting VGF, such as neutralizing anti-VGF mAbs, may offer solutions for patients with EGFR-TKI–resistant lung tumor.

EMT has been linked to EGFR-TKI resistance; however, the mechanism is not known (28, 29, 43). Here we observed that during EGFR-TKI selection, the EMT phenotypic conversion occurs in HCC827GR cells, which contain high levels of *VGF* and *TWIST1*, and HCC827GR cells develop EGFR-TKI resistance in a non-T790M–dependent manner. We found that ectopic expression of *VGF* in HCC827 cells not only confers resistance to EGFR-TKIs but also induces the EMT phenotypic alteration accompanied with *TWIST1* upregulation, whereas other EMT regulators, such as *SNAIL and SLUG*, are not induced by *VGF* expression. TWIST1 has been reported to determine cell fates and regulate normal cell differentiation and EMT (44). In addition, TWIST1 encourages cancer cell survival and dissemination (40, 45). Here, we observed that VGF levels correlate with *TWIST1* expression in primary lung adenocarcinoma. Ectopic expression of VGF induces TWIST1 expression. Moreover, TWIST1 expression facilitates EGFR-TKI resistance and induces the expression of mesenchymal markers. These data indicate that VGF-TWIST1 signaling plays a critical role in EGFR-TKI resistance and EMT.

The human carcinoembryonic antigen (CEA), mainly referred to as CEACAM5 and CEACAM6 with shared antigenic determinants, has been wildly used as a tumor marker in colorectal cancer and lung cancer. CEACAM6 expression is higher than that of CEACAM5 in lung adenocarcinoma (41). However, the use of CEA as a prognostic and predictive marker in lung cancer patients is controversial (46). We observed that *CEACAM6* expression is lost in HCC827GR cells and other independently selected EGFR-TKI–resistant cells, all of which develop EGFR-TKI resistance by a non-T790M pathway (Supplementary Fig. S14C). These data suggest that *CEACAM6* expression may not be a predictive biomarker for the prognosis of EGFR-TKI–resistant tumors driven by a non-T790M pathway. Moreover, *VGF* is negatively correlated with *CEACAM6* expression in the primary lung adenocarcinoma (Supplementary Fig. S14D). We found that *CEACAM6* expression does not correlate with overall survival while *VGF* expression predicted a poor survival not only in lung adenocarcinoma patients but also in the EGFR-mutated subpopulation. Recently, *VGF* is detected in *Synaptophysin*- and/or *Chromogranin A*-positive neuroendocrine breast cancer and in a subgroup of basal-like breast cancer, in which *Chromogranin A* and *Synaptophysin* are absent (36). In this study, we found that *VGF* is expressed in lung neuroendocrine carcinoma and EGFR-TKI–resistant lung adenocarcinoma. We observed that although VGF *Synaptophysin*, *Chromogranin A*, and *Chromogranin B* are highly expressed in neuroendocrine tumors, such as small-cell lung cancer and large-cell neuroendocrine carcinoma, only *VGF* levels correlates with EGFR-TKI resistance in EGFR-mutated lung adenocarcinoma (Fig. 3D; Supplementary Figs. S7–S9). While the transformation toward small-cell lung cancer in resistant EGFR-mutated lung adenocarcinoma has been attributed to the RB loss accompanied with EGFR downregulation (47), none of these alterations occur in HCC827GR and H1975 cells. Moreover, VGF, but not *Chromogranin A* or *Synaptophysin*, correlated with a poor survival in patients with lung adenocarcinoma (Fig. 7C and D; Supplementary Figs. S15 and S16). These findings suggest that VGF expression is not only limited to neuroendocrine cancer cells but also could serve as a prognostic biomarker in patients with lung adenocarcinoma.

Taken together, we found that *VGF* is highly expressed in a subgroup of lung adenocarcinoma and favors EGFR-TKI resistance and EMT, thereby predicting a poor survival. These findings provide new insights for the role of *VGF*, a neurotrophic factor, in lung cancer oncogenesis with the potential to serve as a biomarker and therapeutic target for lung cancer intervention.

Disclosure of Potential Conflicts of Interest

No potential conflicts of interest were disclosed.

Authors' Contributions

Acquisition of data (provided animals, acquired and managed patients, provided facilities, etc.): W. Hwang, Y.-F. Chiu, J.-L. Chang, S.-H. Hsiao, S.-E. Lin

Analysis and interpretation of data (e.g., statistical analysis, biostatistics, computational analysis): W. Hwang, Y.-F. Chiu, M.-H. Kuo, K.-L. Lee, J.-L. Chang, W.-C. Huang, S.-E. Lin

Writing, review, and/or revision of the manuscript: W. Hwang, Y.-F. Chiu, A.-C. Lee, M.-H. Kuo, Y.-T. Chou

Administrative, technical, or material support (i.e., reporting or organizing data, constructing databases): Y.-F. Chiu, A.-C. Lee, C.-C. Yu, J.-L. Chang, W.-C. Huang

Study supervision: Y.-T. Chou

Acknowledgments

We thank Dr. Michael S. Lan (Louisiana State University) for critical reading of this manuscript and insightful comments. We also thank staff at the Eighth

Core Lab, Department of Medical Research, National Taiwan University Hospital, for technical support.

Grant Support

This work was supported by National Tsing Hua University and SMOBiO Inc.

The costs of publication of this article were defrayed in part by the payment of page charges. This article must therefore be hereby marked *advertisement* in accordance with 18 U.S.C. Section 1734 solely to indicate this fact.

Received November 20, 2016; revised January 4, 2017; accepted March 31, 2017; published OnlineFirst April 5, 2017.

References

1. Hsiao SH, Lin HC, Chou YT, Lin SE, Kuo CC, Yu MC, et al. Impact of epidermal growth factor receptor mutations on intracranial treatment response and survival after brain metastases in lung adenocarcinoma patients. Lung Cancer 2013;81:455–61.
2. Pao W, Miller V, Zakowski M, Doherty J, Politi K, Sarkaria I, et al. EGF receptor gene mutations are common in lung cancers from "never smokers" and are associated with sensitivity of tumors to gefitinib and erlotinib. Proc Natl Acad Sci U S A 2004;101:13306–11.
3. Lynch TJ, Bell DW, Sordella R, Gurubhagavatula S, Okimoto RA, Brannigan BW, et al. Activating mutations in the epidermal growth factor receptor underlying responsiveness of non-small-cell lung cancer to gefitinib. N Engl J Med 2004;350:2129–39.
4. Paez JG, Janne PA, Lee JC, Tracy S, Greulich H, Gabriel S, et al. EGFR mutations in lung cancer: correlation with clinical response to gefitinib therapy. Science 2004;304:1497–500.
5. Mok TS, Wu YL, Thongprasert S, Yang CH, Chu DT, Saijo N, et al. Gefitinib or carboplatin-paclitaxel in pulmonary adenocarcinoma. N Engl J Med 2009;361:947–57.
6. Maemondo M, Inoue A, Kobayashi K, Sugawara S, Oizumi S, Isobe H, et al. Gefitinib or chemotherapy for non-small-cell lung cancer with mutated EGFR. N Engl J Med 2010;362:2380–8.
7. Zhou C, Wu YL, Chen G, Feng J, Liu XQ, Wang C, et al. Erlotinib versus chemotherapy as first-line treatment for patients with advanced EGFR mutation-positive non-small-cell lung cancer (OPTIMAL, CTONG-0802): a multicentre, open-label, randomised, phase 3 study. Lancet Oncol 2011;12:735–42.
8. Sequist LV, Yang JC, Yamamoto N, O'Byrne K, Hirsh V, Mok T, et al. Phase III study of afatinib or cisplatin plus pemetrexed in patients with metastatic lung adenocarcinoma with EGFR mutations. J Clin Oncol 2013;31:3327–34.
9. Wu YL, Zhou C, Hu CP, Feng J, Lu S, Huang Y, et al. Afatinib versus cisplatin plus gemcitabine for first-line treatment of Asian patients with advanced non-small-cell lung cancer harbouring EGFR mutations (LUX-Lung 6): an open-label, randomised phase 3 trial. Lancet Oncol 2014;15:213–22.
10. Rosell R, Carcereny E, Gervais R, Vergnenegre A, Massuti B, Felip E, et al. Erlotinib versus standard chemotherapy as first-line treatment for European patients with advanced EGFR mutation-positive non-small-cell lung cancer (EURTAC): a multicentre, open-label, randomised phase 3 trial. Lancet Oncol 2012;13:239–46.
11. Arcila ME, Oxnard GR, Nafa K, Riely GJ, Solomon SB, Zakowski MF, et al. Rebiopsy of lung cancer patients with acquired resistance to EGFR inhibitors and enhanced detection of the T790M mutation using a locked nucleic acid-based assay. Clin Cancer Res 2011;17:1169–80.
12. Kobayashi S, Boggon TJ, Dayaram T, Janne PA, Kocher O, Meyerson M, et al. EGFR mutation and resistance of non-small-cell lung cancer to gefitinib. N Engl J Med 2005;352:786–92.
13. Sequist LV, Waltman BA, Dias-Santagata D, Digumarthy S, Turke AB, Fidias P, et al. Genotypic and histological evolution of lung cancers acquiring resistance to EGFR inhibitors. Sci Transl Med 2011;3:75ra26.
14. Antonicelli A, Cafarotti S, Indini A, Galli A, Russo A, Cesario A, et al. EGFR-targeted therapy for non-small cell lung cancer: focus on EGFR oncogenic mutation. Int J Med Sci 2013;10:320–30.
15. Uramoto H, Yano S, Tanaka F. T790M is associated with a favorable prognosis in Japanese patients treated with an EGFR-TKI. Lung Cancer 2012;76:129–30.
16. Kuiper JL, Heideman DA, Thunnissen E, Paul MA, van Wijk AW, Postmus PE, et al. Incidence of T790M mutation in (sequential) rebiopsies in EGFR-mutated NSCLC-patients. Lung Cancer 2014;85:19–24.
17. Li W, Ren S, Li J, Li A, Fan L, Li X, et al. T790M mutation is associated with better efficacy of treatment beyond progression with EGFR-TKI in advanced NSCLC patients. Lung Cancer 2014;84:295–300.
18. Cross DA, Ashton SE, Ghiorghiu S, Eberlein C, Nebhan CA, Spitzler PJ, et al. AZD9291, an irreversible EGFR TKI, overcomes T790M-mediated resistance to EGFR inhibitors in lung cancer. Cancer Discov 2014;4:1046–61.
19. Ward RA, Anderton MJ, Ashton S, Bethel PA, Box M, Butterworth S, et al. Structure- and reactivity-based development of covalent inhibitors of the activating and gatekeeper mutant forms of the epidermal growth factor receptor (EGFR). J Med Chem 2013;56:7025–48.
20. Janne PA, Yang JC, Kim DW, Planchard D, Ohe Y, Ramalingam SS, et al. AZD9291 in EGFR inhibitor-resistant non-small-cell lung cancer. N Engl J Med 2015;372:1689–99.
21. Walter AO, Sjin RT, Haringsma HJ, Ohashi K, Sun J, Lee K, et al. Discovery of a mutant-selective covalent inhibitor of EGFR that overcomes T790M-mediated resistance in NSCLC. Cancer Discov 2013;3:1404–15.
22. Sequist LV, Soria JC, Goldman JW, Wakelee HA, Gadgeel SM, Varga A, et al. Rociletinib in EGFR-mutated non-small-cell lung cancer. N Engl J Med 2015;372:1700–9.
23. Thress KS, Paweletz CP, Felip E, Cho BC, Stetson D, Dougherty B, et al. Acquired EGFR C797S mutation mediates resistance to AZD9291 in non-small cell lung cancer harboring EGFR T790M. Nat Med 2015;21:560–2.
24. Piotrowska Z, Niederst MJ, Karlovich CA, Wakelee HA, Neal JW, Mino-Kenudson M, et al. Heterogeneity underlies the emergence of EGFRT790 wild-type clones following treatment of T790M-positive cancers with a third-generation EGFR inhibitor. Cancer Discov 2015;5:713–22.
25. Shiao TH, Chang YL, Yu CJ, Chang YC, Hsu YC, Chang SH, et al. Epidermal growth factor receptor mutations in small cell lung cancer: a brief report. J Thorac Oncol 2011;6:195–8.
26. Tatematsu A, Shimizu J, Murakami Y, Horio Y, Nakamura S, Hida T, et al. Epidermal growth factor receptor mutations in small cell lung cancer. Clin Cancer Res 2008;14:6092–6.
27. Kogo M, Shimizu R, Uehara K, Takahashi Y, Kokubo M, Imai Y, et al. Transformation to large cell neuroendocrine carcinoma as acquired resistance mechanism of EGFR tyrosine kinase inhibitor. Lung Cancer 2015;90:364–8.
28. Yauch RL, Januario T, Eberhard DA, Cavet G, Zhu W, Fu L, et al. Epithelial versus mesenchymal phenotype determines in vitro sensitivity and predicts clinical activity of erlotinib in lung cancer patients. Clin Cancer Res 2005;11(24 Pt 1):8686–98.
29. Thomson S, Buck E, Petti F, Griffin G, Brown E, Ramnarine N, et al. Epithelial to mesenchymal transition is a determinant of sensitivity of non-small-cell lung carcinoma cell lines and xenografts to epidermal growth factor receptor inhibition. Cancer Res 2005;65:9455–62.
30. Hahm S, Mizuno TM, Wu TJ, Wisor JP, Priest CA, Kozak CA, et al. Targeted deletion of the Vgf gene indicates that the encoded secretory peptide precursor plays a novel role in the regulation of energy balance. Neuron 1999;23:537–48.
31. Bartolomucci A, La Corte G, Possenti R, Locatelli V, Rigamonti AE, Torsello A, et al. TLQP-21, a VGF-derived peptide, increases energy expenditure and prevents the early phase of diet-induced obesity. Proc Natl Acad Sci U S A 2006;103:14584–9.
32. Severini C, Ciotti MT, Biondini L, Quaresima S, Rinaldi AM, Levi A, et al. TLQP-21, a neuroendocrine VGF-derived peptide, prevents cerebellar granule cells death induced by serum and potassium deprivation. J Neurochem 2008;104:534–44.
33. Shimazawa M, Tanaka H, Ito Y, Morimoto N, Tsuruma K, Kadokura M, et al. An inducer of VGF protects cells against ER stress-induced cell death and prolongs survival in the mutant SOD1 animal models of familial ALS. PLoS One 2010;5:e15307.
34. Rindi G, Licini L, Necchi V, Bottarelli L, Campanini N, Azzoni C, et al. Peptide products of the neurotrophin-inducible gene vgf are produced in human neuroendocrine cells from early development and increase in hyperplasia and neoplasia. J Clin Endocrinol Metab 2007;92:2811–5.

35. Matsumoto T, Kawashima Y, Nagashio R, Kageyama T, Kodera Y, Jiang SX, et al. A new possible lung cancer marker: VGF detection from the conditioned medium of pulmonary large cell neuroendocrine carcinoma-derived cells using secretome analysis. Int J Biol Markers 2009;24:282–5.
36. Annaratone L, Medico E, Rangel N, Castellano I, Marchio C, Sapino A, et al. Search for neuro-endocrine markers (chromogranin A, synaptophysin and VGF) in breast cancers. An integrated approach using immunohistochemistry and gene expression profiling. Endocr Pathol 2014;25:219–28.
37. Chou YT, Lee CC, Hsiao SH, Lin SE, Lin SC, Chung CH, et al. The emerging role of SOX2 in cell proliferation and survival and its crosstalk with oncogenic signaling in lung cancer. Stem Cells 2013;31:2607–19.
38. Lin SC, Chou YT, Jiang SS, Chang JL, Chung CH, Kao YR, et al. Epigenetic switch between SOX2 and SOX9 regulates cancer cell plasticity. Cancer Res 2016;76:7036–48.
39. Chou YT, Hsieh CH, Chiou SH, Hsu CF, Kao YR, Lee CC, et al. CITED2 functions as a molecular switch of cytokine-induced proliferation and quiescence. Cell Death Differ 2012;19:2015–28.
40. Valsesia-Wittmann S, Magdeleine M, Dupasquier S, Garin E, Jallas AC, Combaret V, et al. Oncogenic cooperation between H-Twist and N-Myc overrides failsafe programs in cancer cells. Cancer Cell 2004; 6:625–30.
41. Blumenthal RD, Leon E, Hansen HJ, Goldenberg DM. Expression patterns of CEACAM5 and CEACAM6 in primary and metastatic cancers. BMC Cancer 2007;7:2.
42. Thakker-Varia S, Krol JJ, Nettleton J, Bilimoria PM, Bangasser DA, Shors TJ, et al. The neuropeptide VGF produces antidepressant-like behavioral effects and enhances proliferation in the hippocampus. J Neurosci 2007;27:12156–67.
43. Uramoto H, Iwata T, Onitsuka T, Shimokawa H, Hanagiri T, Oyama T. Epithelial-mesenchymal transition in EGFR-TKI acquired resistant lung adenocarcinoma. Anticancer Res 2010;30:2513–7.
44. Sosic D, Richardson JA, Yu K, Ornitz DM, Olson EN. Twist regulates cytokine gene expression through a negative feedback loop that represses NF-kappaB activity. Cell 2003;112:169–80.
45. Yang J, Mani SA, Donaher JL, Ramaswamy S, Itzykson RA, Come C, et al. Twist, a master regulator of morphogenesis, plays an essential role in tumor metastasis. Cell 2004;117:927–39.
46. Grunnet M, Sorensen JB. Carcinoembryonic antigen (CEA) as tumor marker in lung cancer. Lung Cancer 2012;76:138–43.
47. Niederst MJ, Sequist LV, Poirier JT, Mermel CH, Lockerman EL, Garcia AR, et al. RB loss in resistant EGFR mutant lung adenocarcinomas that transform to small-cell lung cancer. Nat Commun 2015;6:6377.